# Molecular Dynamics of Buspirone Analogues Interacting with the 5-HT$_{1A}$ and 5-HT$_{2A}$ Serotonin Receptors

Agnieszka Bronowska,[a] Andrzej Leś,[a,b] Zdzislaw Chilmonczyk,[c] Slawomir Filipek,[a] Øyvind Edvardsen,[d] Roy Østensen[e] and Ingebrigt Sylte[f,*]

[a]Department of Chemistry, University of Warsaw, Pasteura 1, 02-093 Warsaw, Poland
[b]Pharmaceutical Research Institute, Rydygiera 8, 01-793 Warsaw, Poland
[c]Drug Institute, 30/34 Chelmska Str., Warsaw, Poland
[d]Department of Pharmacology, Institute of Pharmacy, University of Tromsø, N-9037 Tromsø, Norway
[e]Department of Physics, University of Tromsø, N-9037 Tromsø, Norway
[f]Department of Pharmacology, Institute of Medical Biology, University of Tromsø, N-9037 Tromsø, Norway

**Abstract**—Three-dimensional (3-D) models of the human serotonin 5-HT$_{1A}$ and 5-HT$_{2A}$ receptors were constructed, energy refined, and used to study the interactions with a series of buspirone analogues. For both receptors, the calculations showed that the main interactions of the ligand imide moieties were with amino acids in transmembrane helix (TMH) 2 and 7, while the main interactions of the ligand aromatic moieties were with amino acids in TMH5, 6 and 7. Differences in binding site architecture in the region of highly conserved serine and tyrosine residues in TMH7 gave slightly different binding modes of the buspirone analogues at the 5-HT$_{1A}$ and 5-HT$_{2A}$ receptors. Molecular dynamics simulations of receptor-ligand interactions indicated that the buspirone analogues did not alter the interhelical hydrogen bonding patterns upon binding to the 5-HT$_{2A}$ receptor, while interhelical hydrogen bonds were broken and others were formed upon ligand binding to the 5-HT$_{1A}$ receptor. The ligand-induced changes in interhelical hydrogen bonding patterns of the 5-HT$_{1A}$ receptor were followed by rigid body movements of TMH2, 4 and 6 relative to each other and to the other TMHs, which may reflect the structural conversion into an active receptor structure. © 2001 Elsevier Science Ltd. All rights reserved.
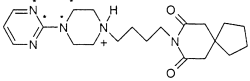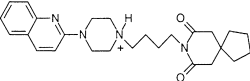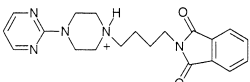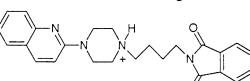
## Introduction

The serotonin receptors (except for the 5-HT$_3$ receptor) are members of the rhodopsin family of G-protein-coupled receptors (GPCRs).[1] Recently, an X-ray crystal structure of rhodopsin at 2.8 Å resolution was reported.[2] This is the first experimental structure of a GPCR at an atomic resolution, and the organisation of the seven transmembrane helices (TMHs) confirms the suggested α-carbon template for the TMHs in the rhodopsin family of GPCRs.[3] GPCRs are integral membrane proteins consisting of seven transmembrane-spanning α-helices (TMHs), connected by three intracellular (Is) and three extracellular (Es) loops forming a central core. The available data indicate that binding of small ligands (neurotransmitters, drugs) to GPCRs involves amino-acids within the central core.[3]

Clinical trials have shown that buspirone, which is structurally unrelated to the benzodiazepines, has anxiolytic and anti-depressive properties.[4–6] Buspirone is a relatively potent but non-selective partial agonist at 5-HT$_{1A}$ serotonin receptors,[4] and its anxiolytic effects are assumed to be related to its 5-HT$_{1A}$ receptor affinity.[4–6] In general, the buspirone analogues have some important advantages over other groups of anxiolytics, such as the benzodiazepines; they do not cause a sedative effect, the toxicity is relatively small, they are not addictive, and they have no associated withdrawal syndrome.[7] The introduction of buspirone as a clinically efficacious anxiolytic drug has focused attention on the 5-HT$_{1A}$ receptor as a possible molecular site for anxiolytic drug action, and several buspirone analogues have been synthesised and tested for their 5-HT$_{1A}$ receptor affinities.[8]

*Corresponding author. Tel.: +47-77-64-4705; fax: +47-77-64-5310; e-mail: sylte@fagmed.uit.no

**Table 1.** Structures and affinity data of buspirone and its analogues. The affinities ($K_i$) towards 5-HT$_{1A}$ and 5-HT$_{2A}$ receptors are given in nmol/dm$^3$. For buspirone, torsional angle N1–C2–N3–C12 is specified by asterisks

| Compound | Structure | $K_i$ (5-HT$_{1A}$) | $K_i$ (5-HT$_{2A}$) |
|---|---|---|---|
| Buspirone (1) | | 14[43] | 794[44] |
| Kaspar (2) | | 39[8] | 3442[14] |
| GL36 (3) | | 36[45] | Not available |
| A7 (4) | | 39[46] | 710[46] |

There are indications that 5-HT$_{2A}$, 5-HT$_{2B}$ and 5-HT$_{2C}$ receptors may also be targets for anxiolytic drugs.[9,10] Mixed 5-HT$_{2A/2C}$ receptor antagonists, like ritanserin, have anxiolytic properties in animal models[11] and in clinical trials.[12] Ligands combining agonist properties at presynaptic 5-HT$_{1A}$ receptors with antagonist properties at 5-HT$_{2A/2C}$ receptors may have greater efficacy than buspirone in producing anxiolytic effects.[13] To rationalise the design of new compounds with a therapeutic potential in the treatment of anxiety, more information about the structural determinates for 5-HT$_{1A}$ and 5-HT$_{2A/2C}$ receptor specific binding, and about the conformational states of the receptor induced by different ligands is necessary.

Computational chemistry techniques have proved to be valuable tools for a better understanding of the molecular events involved in drug specificity and selectivity and for the study of protein dynamics. In the present study, three-dimensional (3-D) models of the human serotonin 5-HT$_{1A}$ and 5-HT$_{2A}$ receptors were constructed by computational chemistry techniques based on the suggested α-carbon template for the TMHs in the rhodopsin family of GPCRs.[3] The models were used to study structural determinants for 5-HT$_{1A}$ and 5-HT$_{2A}$ receptor selectivity of buspirone and three of its analogues (Table 1), and to study the different conformational states of the receptors induced by the buspirone analogues.

## Results

### Conformational analysis of the ligands

In order to obtain low-energy conformers that might interact with the receptors, the conformational space of the ligand molecules (Table 1) were explored by molecular dynamics (MD) simulations. Conformers obtained during MD simulations were analysed, and the conformers with a structure in accordance with the biophore model of the 5-HT$_{1A}$ receptor or the 5-HT$_{2A}$ receptor (Fig. 1) were energy-minimised. The results of the conformational analysis of ligands (1)–(4) (Table 1)

are shown in Table 2. Due to the structural requirements of the biophore model, all these conformers had the *n*-butyl moiety in a strongly bent conformation.

(a)

$d_{N1\text{-}CENT}= 6.4$ Å
$d_{N1\text{-}N2}= 5.0$ Å
$d_{N1\text{-}N3}= 7.2$ Å
$d_{N2\text{-}N3}= 4.8$ Å
$d_{N2\text{-}CENT}= 5.2$ Å

(b)

$d_{N\text{-}O}= 7.9$ Å
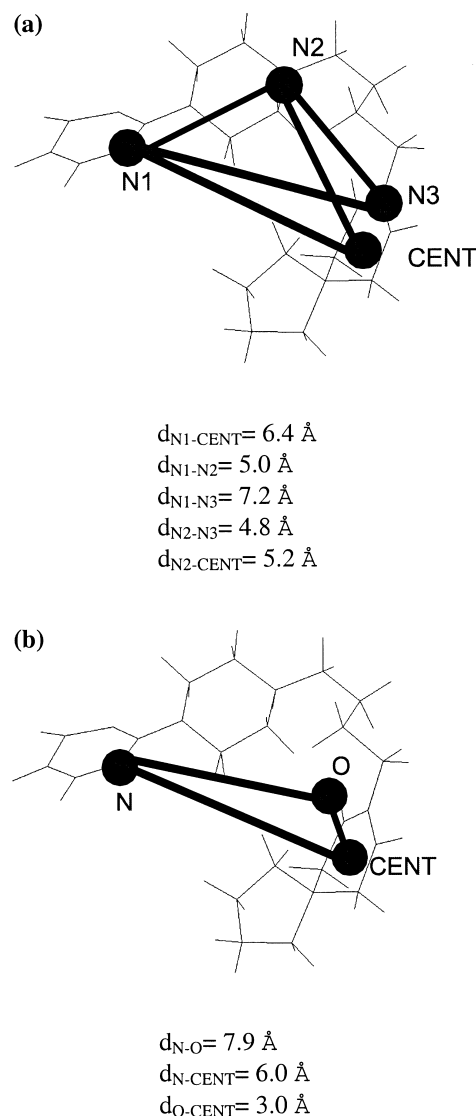$d_{N\text{-}CENT}= 6.0$ Å
$d_{O\text{-}CENT}= 3.0$ Å

**Figure 1.** Biophore models for the (a) 5-HT$_{1A}$ and (b) 5-HT$_{2A}$ receptors.

**Table 2.** Conformational analysis of buspirone analogues. For all conformers of the ligands in agreement with the biphore models: the *N*-butyl moiety in bent conformation, the piperazine ring in chair or twisted chair conformation. $\Delta E$ (chair-boat) conformation of piperazine ring: 0.7–2.0 kcal/mol

| Ligand | Number of conformations in accordance with the 5-HT$_{1A}$ biophore | Number of conformations in accordance with the 5-HT$_{2A}$ biophore | Position of aromatic moiety relative to the piperazine ring[a] | Position of N-butyl moiety relative to the piperazine ring[b] | The range of the torsional angle (N1–C1–N2–C11 (degrees)) between the piperazine and pyrimidine rings |
|---|---|---|---|---|---|
| (<u>1</u>) | > 150 | 80 | Usually equatorial | Usually equatorial | 30–70 |
| (<u>2</u>) | 120 | 30 | Axial | Usually equatorial | 30–90 |
| (<u>3</u>) | 100 | 20 | Axial or equatorial | Usually equatorial | 30–90 |
| (<u>4</u>) | 50 | 50 | Axial or equatorial | Axial or equatorial | 30–70 |

[a] $\Delta E$ (axial-equatorial) substitution of aromatic moiety versus piperazine ring: 0.1–0.5 kcal/mol.
[b] $\Delta E$ (axial-equatorial) substitution of *n*-butyl moiety versus piperazine ring: 0.2–1.2 kcal/mol.

Some of the conformers had the piperazine NH hydrogen atom (Table 1) exposed, while others had this hydrogen atom hidden. Most of the observed conformers in agreement with the biophore models had the piperazine ring in chair or twisted-chair conformation. However, the calculations indicated that the energy difference ($\Delta E$) between chair and boat conformations of the piperazine ring was low for all ligands (Table 2). The torsional angle N1–C2–N3–C12 (Table 1) of conformers that fitted the biophore models indicated a relatively free rotation around the C–N bond between the piperazine ring and the aromatic moiety. Most of the examined conformers had the pyrimidine ring and *n*-butyl moiety in an equatorial position relative to the piperazine ring, but some conformers had the pyrimidine ring ((<u>1</u>), (<u>3</u>) and (<u>4</u>)) and the *n*-butyl moiety (<u>4</u>) in an axial position to the piperazine ring. However, the potential

energy difference ($\Delta E$) between axial and equatorial substitution of the piperazine ring was very low both for the pyrimidine ring and the *n*-butyl moiety (Table 2).

### Structure of the 5-HT$_{1A}$ and 5-HT$_{2A}$ receptor models

The structures of the 5-HT$_{1A}$ and the 5-HT$_{2A}$ receptors after MD simulation of the free receptors are shown in Figure 2. The main purpose of the MD simulations of the free receptors was to obtain conformationally and energetically stable receptor structures. As indicated in Figure 2, the main structural differences between the 5-HT$_{1A}$ and 5-HT$_{2A}$ receptors after MD were in loops and terminal parts. These structural differences may influence the ligand binding process and contribute to affinity differences of various ligands for the 5-HT$_{1A}$ and 5-HT$_{2A}$ receptors.
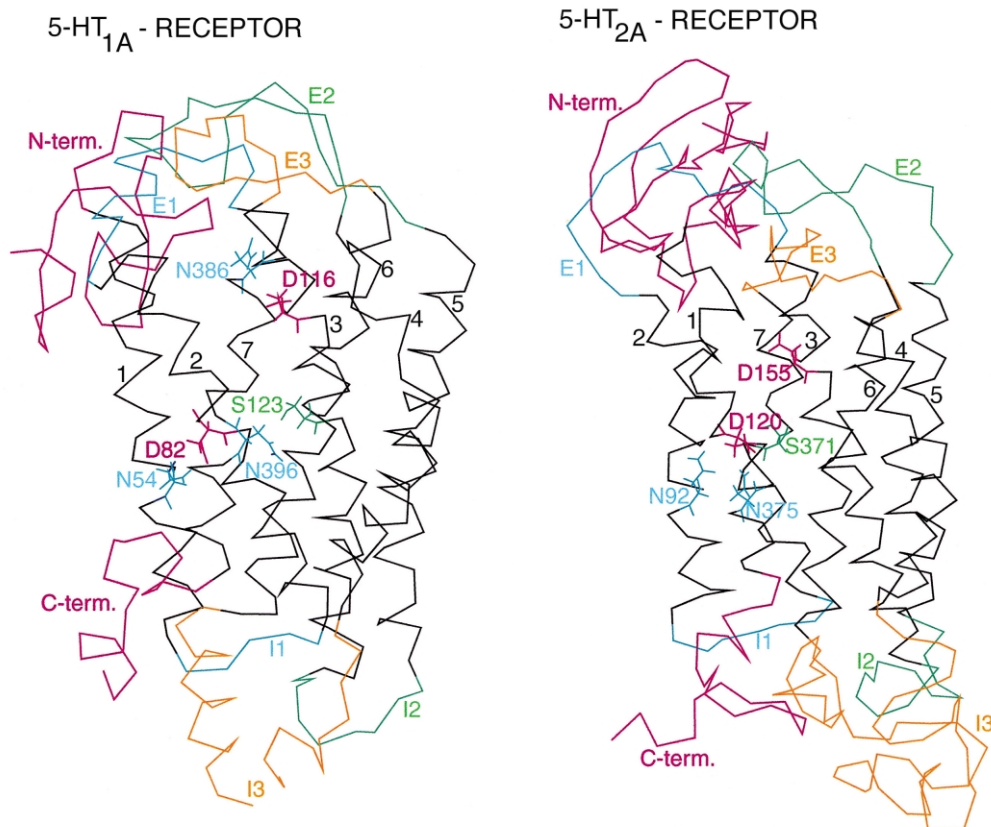


**Figure 2.** Cα-atom traces of the energy-minimised average receptor structures after MD simulations of the free receptor structures. Residues 237–323 in I3 of the 5-HT$_{1A}$ receptor and residues 406–470 in the C-terminal of the 5-HT$_{2A}$ receptor are not shown in the figure.

**Table 3.** Contact residues between the 5-HT$_{1A}$ receptor and the buspirone analogues[a]

| Ligand | Aromatic moiety | Piperazine ring | N-Butyl moiety | Imide moiety |
|---|---|---|---|---|
| Buspirone (1) in position 1 | A50(1), T81(2), D82(2), V85(2), S123(3), F354(6), W358(6), N396(7), P397(7), Y400(7) | L46(1), D116(3), C119(3) C120(3), N392(7), S393(7), N396(7), P397(7) | L43(1), P361(6), L388(7), G389(7) | T39(1), V98(2), I113(3), C109(3), F112(3), A186(E2), C187(E2), L381(7), G382(7), I385(7), N386(7), Y390(7) |
| Buspirone (1) in position 2 | I113(3), V117(3), W175(E2), T196(5), I197(5), T200(5), L366(6), L368(6), L381(7) | D116(3), V117(3), C120(3), F204(5), F361(6), L366(6), I385(7) | D116(3), C120(3), W358(6), G389(7), S393(7) | L88(2), N100(2), F112(3), N386(7), Y390(7), S393(7) |
| Kaspar (2) in position 1 | S123(3), I124(3), I127(3), W358(6), F361(6), S393(7), N396(7) | V85(2), D116(3), C119(3), C120(3), F361(6), G389(7), N392(7), S393(7) | V85(2), L88(2), N386(7), Y390(7) | L46(1), M84(2), T81(2), D82(2), V85(2), L88(2), V89(2), F112(3), L115(3), N386(7), Y390(7) |
| Kaspar (2) in position 2 | G174(4), W175(E2), T188(E2), H193(5), L381(7), G382(7), I385(7) | D116(3), V117(3), C120(3), F204(5), F361(6), G389(7) | D116(3), C120(3), G389(7), N386(7), Y390(7), S393(7) | L46(1), L88(2), Val89(2), M92(2), F112(3), I113(3), D116(3), Y390(7), S393(7) |
| A7 (4) in position 1 | T81(2), C120(3), S123(3), I124(3), L127(3), F354(6), W358(6), N392(7), S393(7), N396(7) | L88(2), V85(2), D116(3), C119(3), C120(3) | L46(1), V85(2), L88(2), V89(2), G389(7), Y390(7), S393(7) | L88(2), V89(2), M92(2), C109(3), F112(3), I113(3), D116(3), C187(E2), I385 (7), N386(7) |
| A7 (4) in position 2 | H193(5), A365(6), P369(6), L381(7), | I113(3), D116(3), F361(6), I385(7), | C120(3), G389(7), Y390(7) | L46(1), L88(2), V89(2), M92(2), F112(3), V117(3), Y390(7), S393(7) |
| GL36 (3) in position 1 | T81(2), D82(2), C119(3), C120(3), S123(3), W358(6), N392(7), S393(7), N396(7) | V85(2), L88(2), D116(3), G389(7), S393(7) | L88(2), V89(2), M92(2), G389(7), Y390(7) | V98(2), L99(2), N100(2), C109(3), F112(2), I113(2), L381(3), G382(3), I385(7), N386(7) |
| GL36 (3) in position 2 | G174(4), W175(E2), R176(E2), T188(E2), I197(5), L381(7), G382(7) | I113(3), D116(3), V117(3), T200(5), F204(5), I385(7) | C120(3), F204(5), F361(6), N386(7), G389(7) | V85(2), L88(2), V89(2), M92(2), D116(3), C119(3), Y390(7), S393(7) |

[a]Ligand–receptor contact residues in the energy minimized average complexes between 140 and 170 ps. Amino acids with van der Waals contacts with the ligands and other amino acids close to the ligand (contact after 20% increased van der Waals radii) are included in the table. TMHs are indicated by numbers. E1–E3 indicates the extracellular loops. Standard one-letter abbreviations are used for the amino acids.

The interhelical hydrogen-bonding pattern is slightly different between the 5-HT$_{1A}$ and 5-HT$_{2A}$ receptors (Fig. 2), which give small structural differences in the helical packing and the active site geometry of the receptors. The energy-minimised average structure after MD of the free 5-HT$_{1A}$ receptor possesses hydrogen bonds between: Asn54(TMH1)–Asp82(TMH2), Asp82(TMH2)–Pro397(TMH7), Ser123(TMH3)–Ser393-(TMH7), Ser123(TMH3)–Asn396(TMH7) and Asp116-(TMH3)–Asn386(TMH7). Except for Asn386, these amino acids are highly conserved in the rhodopsin family of GPCRs. Ligand-induced changes in the hydrogen bonding pattern may play a crucial role in G-protein activation and signal transduction. In the energy-minimised average structure after MD of the free 5-HT$_{2A}$ receptor, a corresponding hydrogen bonding pattern was between: Asn92(TMH1)–Asp120(TMH2), Asp120(TMH2)–Ser371(TMH7), Asp120(TMH2)–Ser372-(TMH7), Asp120(TMH2)–Asn375(TMH7) and Ser162-(TMH3)–Ser371(TMH7). Except for Ser371, these amino acids are also highly conserved in the rhodopsin family of GPCRs.

**Buspirone analogues–5-HT$_{1A}$ receptor interactions**

The amino acids in close contact with the ligands in the energy-minimised average complexes after MD simulations are shown in Table 3. These close van der Waals contacts may be interpreted as the main contributors to ligand–receptor interactions. At the start of all simulations, the ligand conformers (Fig. 3) were placed in the central cavity of the receptor with the protonated amino group in close vicinity of Asp116(TMH3). Strong interactions were maintained between Asp116 and the protonated amino group during all simulations of receptor–ligand complexes.

After MD in both positions the location of the quinolinyl derivatives (2 and 4) was slightly different from the position of the pyrimidinyl derivatives (1 and 3). In position 2, the aromatic moieties of (2) and (4) interacted closer to the extracellular side of the receptor than did (1) and (3) (Fig. 5), and relatively strong interactions with amino acids in E2 and TMH4 were seen (Table 3). Such interactions were not observed for the pyrimidinyl derivatives.

**Ligand-induced conformational changes of the 5-HT$_{1A}$ receptor**

Comparison of the receptor structures after MD of the free receptor and of the receptor–ligand complexes may give insight into the structural changes of the receptors induced by the buspirone analogues. After MD simulation of the ligand–5-HT$_{1A}$ complexes, some interesting effects were observed:

1. Large conformational change of all ligands during simulation in position 1. The initial bent conformation (in accordance with the biophore model in Fig. 1) became much more extended during MD. Similar conformational changes were not observed during MD with the buspirone analogues in position 2.
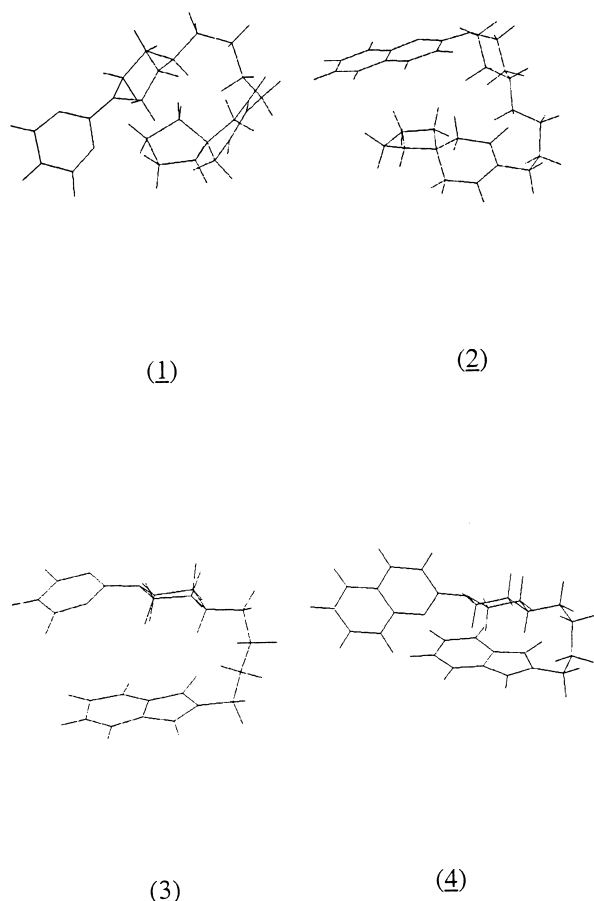
(1)   (2)

(3)   (4)

**Figure 3.** The low-energy conformers of the ligands used in the MD simulations of ligand–receptor interactions.

2. Compared with the structure after MD of the free 5-HT$_{1A}$ receptor, the buspirone analogues induced displacements of TMHs 2, 4, and 6 in position 2, and in all TMHs in position 1 (Table 5).
3. Compared with the structure after MD with the free receptor, the buspirone analogues also induced structural changes into I2 and I3. These ligand-induced structural changes were particularly large after MD with (1) in position 2, and especially the fragments Arg223(I3)–Ile226(I3) and Glu322(I3)–Arg339(I3) were affected. In the model, Glu322(I3)–Arg339(I3) is a short helix connected to the intracellular end of TMH6. This helix is located much closer to I2 after MD with (1) in position 2 than after MD of the free receptor structure. However, the helix is more accessible from the cytosol after MD of the free receptor than after MD with (1).

The buspirone analogues also influenced the interhelical hydrogen bonding patterns between amino acids in TMH2, 3 and 7, that was present in the receptor after MD with the free receptor. After MD with the buspirone analogues in postion 1, the following hydrogen bonds that were present after MD of the unbound receptor were broken: Ser123(TMH3)–Asn396(TMH7) (ligand (1)), Ser123(TMH3)–Ser393(TMH7) (all ligands), Asp82(TMH2)–Pro397(TMH7) (all ligands) and Asp116(TMH3)–Asn386(TMH7) (all ligands). The following hydrogen bonds were created: Asp82(TMH2)–Asn396(TMH7) (all ligands), Thr81(TMH2)–Ser123(TMH3) (ligands (1), (3) and (4)), Thr81(TMH2)–Asn396(TMH7) (ligand (1)). Ligands (1) and (2) also attenuated the

**Table 4.** Contact residues between the 5-HT$_{2A}$ receptor and the buspirone analogues[a]

| Ligand | Aromatic moiety | Piperazine ring | N-Butyl moiety | Imide moiety |
|---|---|---|---|---|
| Buspironen (1) in position 1 | T88(1), D120(2), L123(2), G124(2), S371(7), V374(7), N375(7) | L123(2), D155(3), G339(6) | L126(2), V127(2), V130(2), I367(7) | F364(7), L126(2), V130(2), I152(3), W151(3), I343(6), A359(7), L360(7), V363(7) |
| Buspirone (1) in position 2 | C148(3), I152(3), Cys227(5), N342(6), I343(6), V346(6), I347(6), I357(7), G358(7), A359(7), V363(7) | W151(3), I152(3), D155(3), L360(6), F364(7), I367(7) | L126(2), V127(2), V130(2), F364(7) | L123(2), L126(2), S159(3), W151(3), E339(6), I367(7), G368(7), L370(7), S371(7) |
| Kaspar (2) in position 1 | V84(1), T88(1), D120(2), L123(2), G124(2), V127(2), G368(7), S371(7), S372(7) | D155(3), S159(3), F364(7), I367(7) | I343(6), G358(6) | I163(3), F240(5), C336(6), E339(6), I340(6) |
| Kaspar (2) in position 2 | I152(3), D155(3), L236(5), I237(5), F240(5), I343(6), I347(6), G358(7), A359(7), V363(7) | I152(3), D155(3), V156(3), F364(7), I367(7) | L123(2), V127(2), I367(7), G368(7) | V47(NT), D48(NT), S77(1), T81(1), L123(2), V127(2), V130(2), L360(7), L361(7) |
| A7 (4) in position 1 | V84(1), T88(1), D120(2), L123(2), I367(7), L370(7), S371(7), V374(7), N375(7) | L126(2), V127(2), D155(3), F364(7), I367(7), | V130(2), L228(E2), L360(7), V363(7), | I152(3), D155(3), V156(3), S159(3), L228(E2), F240(5), F243(5), I343(6) |
| A7 (4) in position 2 | L126(2), V127(2), S131(2), W151(3), I152(3), D155(3), L360(7), F364(7), Gly368(7) | I152(3), D155(3), V156(3), F240(5), E339(6), I340(6), I343(6) | S159(3), F243(5), L370(7) | T81(1), V84(1), I85(1), T88(1), L123(2), I367(7), G368(7), L370(7), S371(7) |
| GL36 (3) in position 1 | S159(3), S162(3), S371(7), V374(7), N375(7) | D155(3), V84(1), T88(1), L123(2) | L126(2), V130(2), L360(7), F364(7) | W151(3), I152(3), D155(3), I343(6), I347(6), A359(7), L360(7), V363(7) |
| GL36 (3) in position 2 | L126(2), V130(2), W151(3), L154(3), D155(3), F158(3) | V84(1), V127(2), I152(3), D155(3), L360(7) | V84(1), V363(7), F364(7), I367(7) | L87(1), T88(1), L123(2), S159(3), S162(3), S371(7), V374(7), N375(7) |

[a]Receptor–ligand contacts in the energy-minimised average complexes between 140 and 170 ps. Amino acids with van der Waals contacts with the ligands and other amino acids close to the ligand (contact after 20% increased van der Waals radii) are included in the table. TMHs are indicated by numbers. E1–E3 indicates the extracellular loops. Standard one-letter abbreviations are used for the amino acids.

hydrogen bond Asn54(TMH1)–Asp82(TMH2), but the bond was not broken.

After MD of all buspirone analogues in position 2, the following hydrogen bonds present after MD of the unbound receptor were broken: Ser123(TMH3)–Ser393(TMH7) (all ligands), Ser123(TMH3)–Asn396-(TMH7) (all ligands), Asp82(TMH2)–Pro397(TMH7) (all ligands) and Asp116(TMH3)–Asn386(TMH7) (ligands (1) and (2)). The following hydrogen bonds were created: Thr81(TMH2)–Ser123(TMH3) (all ligands), Asp82(TMH2)–Asn396(TMH7) (ligands (1), (2) and (4)) and Thr81(TMH2)–Asn396(TMH7) (all ligands).

For all complexes, the hydrogen bond between Asn54(TMH1) and Asp82(TMH2) was conserved during MD. These changes in interhelical hydrogen bonding patterns upon ligand binding may be connected to the mechanisms of action of the buspirone analogues.

The potential energy of the receptor upon ligand binding increased more with the ligands in position 1 than in position 2 (Table 6). In position 1, the potential energy upon binding increased in the rank order: (1) < (2) < < (3) < (4), and in position 2 in the rank order: (1) < < (3) < (2) < < (4). Table 6 shows that the binding of (2) increased the potential energy of the receptor
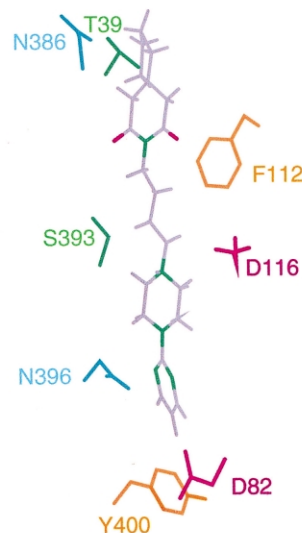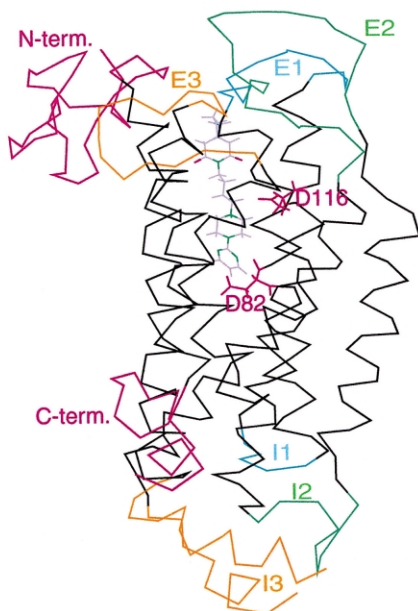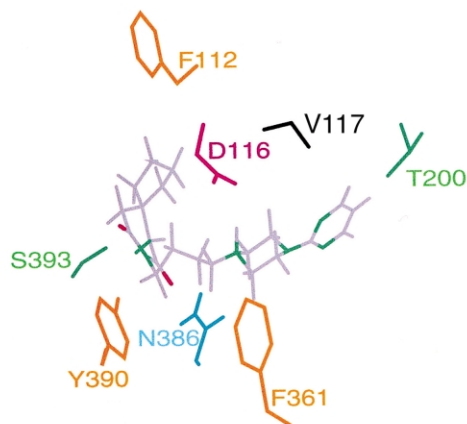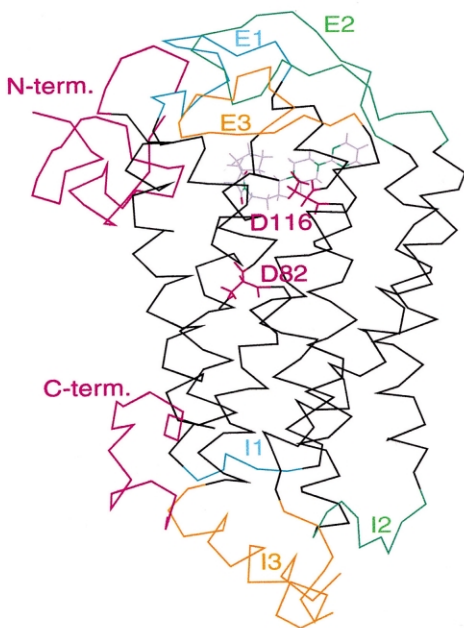


**Figure 4.** Cα-atom traces of energy-minimised average (1)–5-HT$_{1A}$ receptor complexes after MD simulations. Left: the complexes seen in the membrane plane. Residues 237–323 in I3 are not shown. Right: Closer view of the binding sites with (1) nitrogen atoms in green and (1) and oxygen atoms in red.

**Table 5.** The root mean square (r.m.s.) differences of TMHs (backbone atoms) between the energy minimised average 5-HT$_{1A}$ receptor structure after MD of the free receptor and the receptor structures after MD of ligand–5-HT$_{1A}$ receptor interactions. The complexes were averaged over 140–170 ps of simulation

| Helix no. | Free receptor-(1) | | Free receptor-(2) | | Free receptor-(3) | | Free receptor-(4) | |
|---|---|---|---|---|---|---|---|---|
| | Position 1 | Position 2 | Position 1 | Position 2 | Position 1 | Position 2 | Position 1 | Position 2 |
| 1 | 1.0 | 0.8 | 1.1 | 1.4 | 1.6 | 1.0 | 1.6 | 0.9 |
| 2 | 1.4 | 1.6 | 1.6 | 1.7 | 1.7 | 1.8 | 1.4 | 2.0 |
| 3 | 1.5 | 0.9 | 1.5 | 1.1 | 0.9 | 1.3 | 1.3 | 1.1 |
| 4 | 2.1 | 2.5 | 2.2 | 1.8 | 2.2 | 1.8 | 1.8 | 2.6 |
| 5 | 1.2 | 0.7 | 1.0 | 1.4 | 1.1 | 1.3 | 0.6 | 1.0 |
| 6 | 1.3 | 1.6 | 1.0 | 1.8 | 1.6 | 1.4 | 1.2 | 1.7 |

more than did (1), and (4) more than did (3). This may indicate that upon binding the aromatic quinolinyl moiety of (2) and (4) induced a more unfavourable receptor conformation than the aromatic pyrimidyl moiety of (1) and (3). Table 6 also shows that the binding of (4) increased the potential energy of the receptor more than did (2), and (3) more than did (1). This may indicate that upon binding, the phthalimide moiety of (3) and (4) induced a more unfavourable receptor conformation than the imide moiety of (1) and (2).

## Ligands–5-HT$_{2A}$ interactions

At the start of all MD simulation of buspirone analogues–5-HT$_{2A}$ receptor complexes, the compounds were placed in the central core of the receptor with the protonated amino group (Table 1) in close vicinity to Asp155(TMH3). The amino acids in close contacts with the ligands in the energy-minimised average complex after simulations in both positions are shown in Table 4.

The simulations of receptor–ligand interactions indicated that some amino acids are important for binding in both positions. These are: Leu123(TMH2) and Ser371(TMH7) that interact with the aromatic moiety in position 1 and the imide moiety in postion 2, Asp155(TMH3) which interacts with the protonated amino group of the piperazine ring in both positions, and Val127(TMH2), Phe364 (TMH7), Ile367(TMH7), Trp151(TMH3).

In position 1, the initial bent conformation of (1) (Fig. 3) was changed into a more extended conformation during the simulation, while in position 2 the conformation of (1) was very similar to the initial bent conformation. The conformation of (1) after MD in position 1 was quite similar to the extended structure in the X-ray crystal structure of 4,4-dimethyl-1-{4-[4-2-quinolinyl)-1-piperazinyl]butyl}-2,6-piperidinedione and other buspirone analogues.[14] Similar conformational changes were also seen for (3) and (4) during MD in
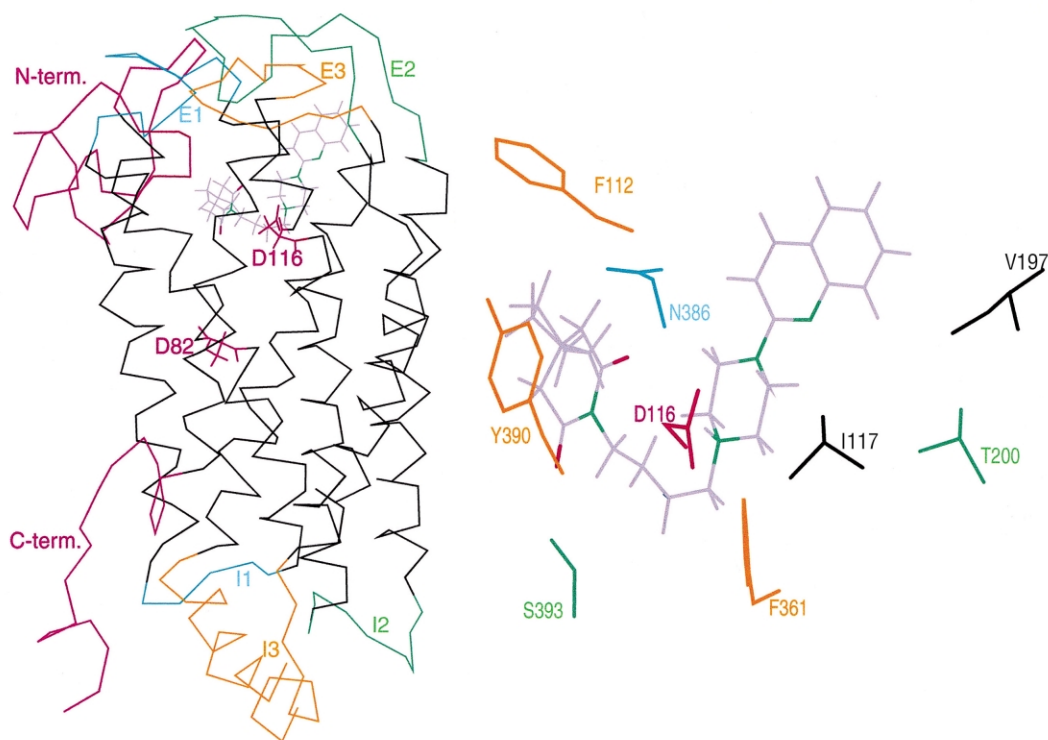


**Figure 5.** Cα-atom trace of the energy-minimised average (2)–5-HT$_{1A}$ receptor complex in positon 2 after MD simulations. Left: the complex seen in the membrane plane. Residues 237–323 in I3 are not shown. Right: Closer view of the ligand binding site with (2) nitrogen atoms in green and (2) oxygen atoms in red.

position 1, but not for (2). After the simulation of (2) in position 1 the ligand was rather bent and very similar to its initial conformation (Fig. 6).

**Ligand-induced conformational changes of the 5-HT$_{2A}$ receptor**

In contrast to the simulations of the 5-HT$_{1A}$ receptor, none of the simulations of ligand interactions with the 5-HT$_{2A}$ receptor caused significant displacement of the TMHs relative to the structure from the simulation with the free receptor. However, some changes in the hydrogen bonding pattern in the region of Asp120(TMH2) and Asp155(TMH3) were observed during MD with (1) in both positions. Some of the hydrogen bonds constraining the TMHs relative to each other were broken but, in contrast to MD with the 5-HT$_{1A}$ receptor, new hydrogen bonds were not formed. During MD of (1) in position 1 the interhelical hydrogen bonds Asp120-(TMH2)–Ser371(TMH7), Ser162(TMH3)–Ser371(TMH7) and Asp120(TMH2)–Ser372, that were present in the free receptor structure were broken, while the simula-
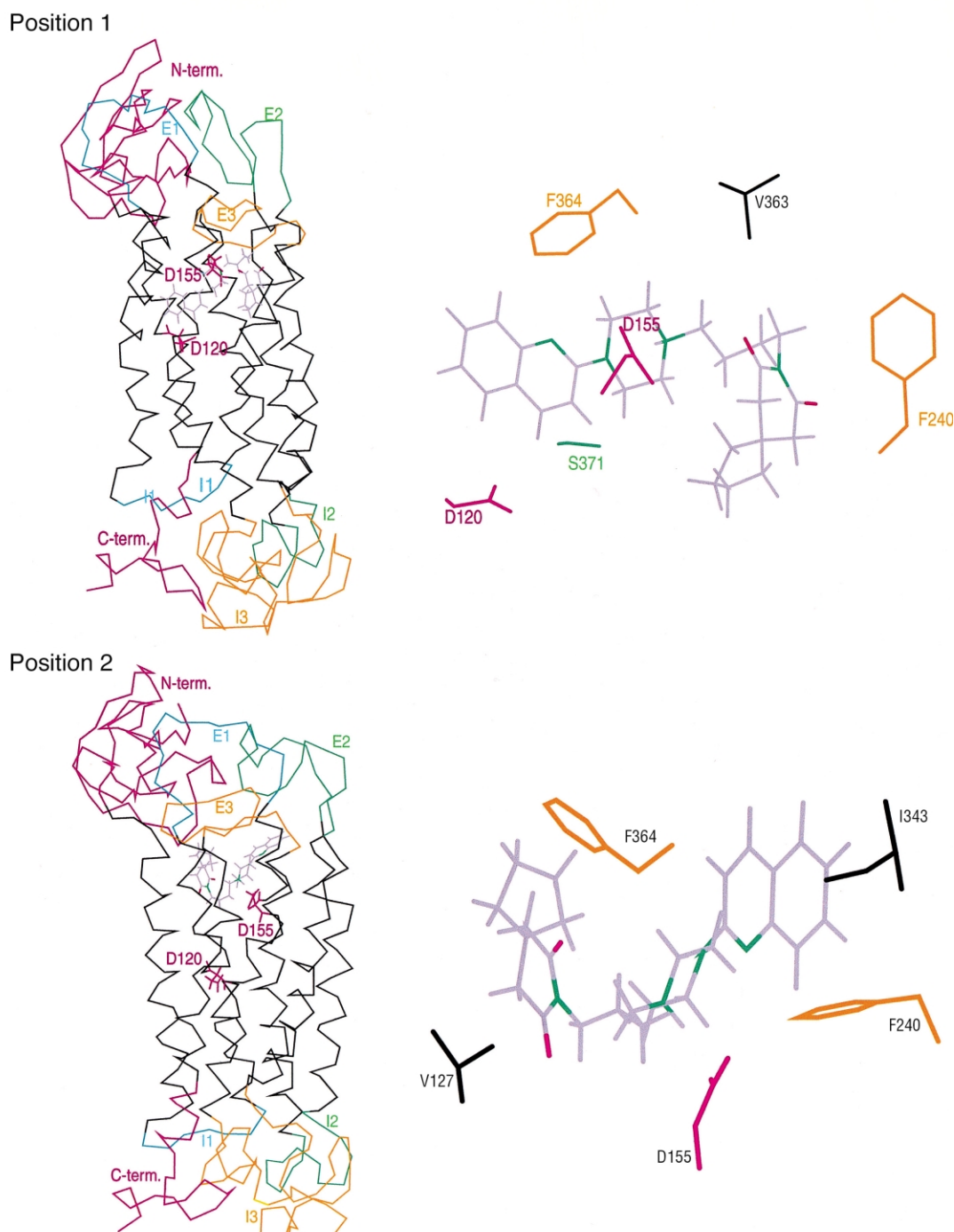


**Figure 6.** Cα-atom traces of energy-minimised average (2)–5-HT$_{2A}$ receptor complexes after MD simulatons. Left: the complexes seen in the membrane plane. Residues 406–470 in the C-terminus are not shown. Right: A closer view of the ligand binding sites in both positions with (2) nitrogen atoms in green and (2) oxygen atoms in red.

**Table 6.** The distortion energy of the 5-HT$_{1A}$ receptor upon ligand binding[a]

| Ligand | Distortion energy (kcal/mol) | |
|---|---|---|
| | Position 1 | Position 2 |
| (1) | 79 | 33 |
| (2) | 85 | 60 |
| (3) | 107 | 59 |
| (4) | 110 | 86 |

[a]The distortion energy is calculated as the difference in potential energy between the receptor structure in the energy-minimised average complex after MD and the separately energy-minimised receptor structure.

tion with (1) in position 2 broke the hydrogen bonds Asp120(TMH2)–Ser371(TMH7) and Asp120(TMH2)–Ser372(TMH7). However, these changes of the interhelical hydrogen bonding pattern in the region of Asp120(TM2) and Asp155(TMH3) were not enough for inducing helical displacement relative to the free receptor as observed during MD of 5-HT$_{1A}$–ligand interactions.

Receptor-induced conformational changes of (2) were not observed at all. During simulations of both (2)–5-HT$_{2A}$ complexes, the interhelical hydrogen bonding pattern between amino acids in TMH2, TMH3 and TMH7 was also similar to that after the simulation with the free 5-HT$_{2A}$ receptor. During simulations with (3) in position 2, minor helical displacements relative to the structure after MD with the free receptor were observed. Ligand (4) behaved very similar to (1) in both positions, and the ligand-induced conformational changes of the receptor during MD were small.

## Discussion

The present models of 5-HT$_{1A}$ and 5-HT$_{2A}$ serotonin receptors were constructed with the helical parts organised according to the suggested α-carbon atom template of GPCRs.[3] This template was confirmed by the recent experimental X-ray structure of bovine rhodopsin at 2.8 Å resolution.[2] At 2.8 Å resolution, it is not possible to identify internal hydrogen bonds and side-chain torsional angels from the X-ray density map, and the experimental model must be considered as relatively crude. Several models of GPCRs have been constructed using detailed atomic structures of bacteriorhodopsin[15–17] as a template. However, there are differences between the structure of bacteriorhodopsin and visual rhodopsin. The TMHs in bacteriorhodopsin are slightly more elongated than in visual rhodopsin.[2,16] In visual rhodopsin, TMH-bundle and 5 are closer to 7 than in bacteriorhodopsin, so that the influence of amino acids in TMH7 on ligand binding may be partly ignored when bacteriorhodopsin is used as a template. The final results of modelling the ligand–receptor interactions and the ligand-induced conformational changes of GPCRs are strongly dependent on the initial model of the receptor. The structural differences between rhodopsin and bacteriorhodopsin suggest that further modeling of GPCRs should be based on the available 2.8 Å resolution structure of visual rhodopsin[2] in spite of available low resolution X-ray crystal structures of bacteriorhodopsin.[16,17]

### The receptor structures

In the energy-minimised average structure after MD of the unbound 5-HT$_{1A}$ and 5-HT$_{2A}$ receptors a hydrogen bonding pattern constrained TMH1, 2, 3, and 7 relative to each other (Fig. 2). The most central amino acids in this hydrogen bonding pattern were an asparagine in TMH1 (Asn54 in 5-HT$_{1A}$, Asn92 in 5-HT$_{2A}$) aspartic acid in TMH2 (Asp82 in the 5-HT$_{1A}$ receptor, Asp120 in 5-HT$_{2A}$) and asparagine in TMH7 (Asn396 in 5-HT$_{1A}$, Asn375 in 5-HT$_{2A}$). These amino acids are highly conserved in the rhodopsin family of GPCRs, and several site-directed mutagenesis studies have suggested that they are involved in a common hydrogen bonding network involved in agonist-induced receptor activation.[18–20] During MD of the unbound 5-HT$_{1A}$ receptor hydrogen bonds were also induced between Asn386(TMH7) and Asp116(TMH3), and between Ser123(TMH3) and Asn396(TMH7). The 5-HT$_{2A}$ receptor has a valine (Val363) corresponding to Asn386(TMH7) of the 5-HT$_{1A}$ receptor, while Asp116 (Asp155 in 5-HT$_{2A}$) and Ser123 (Ser162 in 5-HT$_{2A}$) are highly conserved in the rhodopsin family of GPCRs. After MD of the unbound 5-HT$_{2A}$ receptor hydrogen bonds were formed between Ser162(TMH3) and Ser371(TMH7), and between Asn375(TMH7) and Asp120(TMH2). Therefore, these data suggest that the highly conserved Ser123(TMH3) (Ser162 in the 5-HT$_{2A}$ receptor) might be involved in a common hydrogen-bonding network, structurally important for a proper ligand recognition and receptor activation, and should be experimentally tested for its role in ligand recognition and signal transduction.

The differences in hydrogen bonding pattern in the region of TMH2, 3 and 7 between the unbound 5-HT$_{1A}$ and 5-HT$_{2A}$ receptors contribute to small differences in the active site geometry between the 5-HT$_{1A}$ and 5-HT$_{2A}$ receptors. The hydrogen bond Asp116(TMH3)–Asn386(TMH7) gives the unbound 5-HT$_{1A}$ receptor a much more narrow structure in the region of the aspartic acid in TMH3 than the unbound 5-HT$_{2A}$ receptor. These structural differences at the active site might influence the mechanisms of ligand recognition and binding, and contribute to the differences in affinity for the buspirone analogues.

### Ligand-induced structural changes of the receptor models

A classical model of receptor activation proposes that GPCRs exist in equilibrium between two interconvertible allosteric states (R and R$^*$). The inactive state R predominates in the absence of agonists, due to structural constrains that prevents G-protein activation. In the active state (R$^*$) these constraints are relaxed and the G-protein can interact. The equilibrium between the active and non-active states can be altered by agonist binding or mutations of the receptor.[21–23] These alterations are responsible for the various levels of GPCR activity. The average structures from the MD simulations

provide information about the most populated receptor states in the conformational space explored by the simulation. Therefore, comparing the receptor structures after MD of the free receptor and of the receptor–ligand complexes may give insight into the structural changes induced by the buspirone analogues. These changes may be correlated with the transition from the non-active to the active state of the receptor.

During MD of receptor–ligand interactions the interhelical hydrogen bonding pattern of the 5-HT$_{1A}$ receptor was affected by all the buspirone analogues. Some hydrogen bonds were broken, while others were formed. This suggests that ligand–receptor interactions induce creation or breaking of hydrogen bonds that influence the hydrogen-bonding network constraining TMH1, 2, 3 and 7 relative to each other. The root mean square (r.m.s.) differences of TMHs between the receptor structures after MD of free 5-HT$_{1A}$ receptor and MD with ligands in position 2 indicate that the main differences between these receptor structures are in TMH2, 4 and 6. Inspection of the structures indicated that TMH2, 4 and 6 of the ligand bound receptor structures moved as rigid bodies relative to the structure after MD with the free receptor. The largest r.m.s. difference between the receptor structure after MD of the free receptor and MD with ligands in position 1 was in TMH4 (Table 5). However, in contrast to ligands in position 2, no clear trends in the helical r.m.s. differences relative to the free receptor structure were seen. These observations indicate that the buspirone analogues in position 2 induced movements of TMH2, 4 and 6 relative to the other TMHs, and thereby, induced larger structural changes into the overall architecture of the helical bundle than did ligands in position 1. This favours position 2 in front of position 1 as the most realistic position of the buspirone analogues at the 5-HT$_{1A}$ receptor, and might indicate that partial agonists like buspirone function by inducing rigid body movements of TMH2, 4 and 6 relative to other the TMHs. Rigid body movments of TMHs have previously been observed in the light activation of rhodopsin,[24] and rigid body movments of TMH6 has also been suggested to occur in the activation of the muscarininc M2 receptor.[25] Further, experimental studies have also indicated that agonist induced conformational changes in TMH6 is underlying activation of the $\beta_2$-receptor.[26]

During MD of ligands with the 5-HT$_{2A}$ receptor model, the buspirone analogues were not able to affect the interhelical hydrogen bonding pattern as in the 5-HT$_{1A}$ receptor, and helical displacements relative to the receptor structure after MD of the free 5-HT$_{2A}$ receptor were hardly seen. Ligands (1), (3) and (4) were able to break some of the interhelical hydrogen bonds constraining TMH1, 2 and 7 relative to each other. However, any new interhelical hydrogen bonds between these helices were not formed in the ligand–5-HT$_{2A}$ receptor complexes. After MD of the 5-HT$_{2A}$ receptor complex with compound (2), the interhelical hydrogen bonding patterns were unchanged. During simulations with the 5-HT$_{1A}$ receptor, ligand-induced structural changes were also observed in I2 and I3, especially after MD with ligands in position 2. These ligand-induced

conformational changes in I2 and I3 of the 5-HT$_{1A}$ receptor may reflect the structural conversions of I2 and I3 into a proper structure for G-protein interactions. Some of the buspirone analogues also induced structural changes into I2 and I3 of the 5-HT$_{2A}$ receptor. However, these changes were smaller than for the 5-HT$_{1A}$ receptor. The differences in ligand-induced structural changes in the TMHs, I2 and I3 between the 5-HT$_{1A}$ and 5-HT$_{2A}$ receptors might reflect the lower affinity of the buspirone analogues for the 5-HT$_{2A}$ receptor than for the 5-HT$_{1A}$ receptor.

**Ligand- 5-HT$_{1A}$ receptor interactions**

The most widely-accepted model of ligand binding to GPCRs suggests that the protonated amino group of the ligand interacts with the aspartic acid in TMH3, while other parts of the ligand interact with amino acids closer to the synaptic end of TMH5, 6 and 7.[27] In this model, the highly conserved aspartic acid in TMH2 is not directly involved in ligand binding, but is believed to be important for the structure and function of the receptor. Position 2 of the buspirone analogues are in accordance with this model. An alternative model suggests that the ligands interact closer to the intracellular end of the TMHs, with the highly conserved aspartic acid in TMH2 directly involved in ligand binding, and that the binding pocket consists of residues in TMH2, 3 and 7.[28] Position 1 of the buspirone analogues is more in accordance with this model.

Amino acids that possess close van der Waals contacts and/or interact via hydrogen bonds with the ligands after MD are shown in Table 3. This table indicates that some binding site amino acids are common for both positions. These are: Asp116 (TMH3), Ser393(TMH7), Cys120(TMH3), Gly389(TMH7), Tyr390(TMH7), Val85(TMH2), Val88(TMH2), and Ile385(TMH7). Site directed mutagenesis experiments have indicated that Ser393 is important for binding of 8-hydroxy-2-(diprolyl amino)tetralin (8-OH-DPAT) to the 5-HT$_{1A}$ receptor,[29] while Asp116 correspond to the highly conserved amino acid found to be important for ligand binding in all monoamine GPCRs. Site directed mutagenesis studies have also indicated that Asp82(TMH2) is important for the binding of serotonin to the 5-HT$_{1A}$ receptor,[30] while Asn396(TMH7) is important for binding of 8-OH-DPAT.[29] Asp82 and Asn396 were involved in the interhelical hydrogen bonding pattern constraining TMH2 and 7 relative to each other. These amino acids seem important for proper ligand recognition and signal transduction, and are also directly involved in ligand binding in position 1. Site directed mutagenesis studies have also shown that Ser199(TMH5) and Thr200-(TMH5) are important for binding of serotonin to the 5-HT$_{1A}$ receptor,[30] and that residues in TMH5 and 6 in the 5-HT$_{2A}$ receptor are involved in ligand binding.[31–35] In both positions, several amino acids in TMH5 and 6 were involved in ligand binding (Table 3). Therefore, based on available mutagenesis data, it is not possible to favour one of the two positions over the other. Site-directed mutagenesis studies indicated that an Asn386(TMH7) to valine mutation only had minor

effects on the affinity of buspirone and ipsapirone for the 5-HT$_{1A}$ receptor.[36] In position 1, the side chain of Asn386 interacts with the imide moiety of the buspirone analogues, while the backbone of Asn386(TMH7) interacts with the imide moiety after MD with ligands in position 2. In position 2, a direct buspirone interaction with the backbone of Asn386(TMH7), independent of the side chain of this residue, was observed, and is therefore in accordance with mutagenesis data and might favour position 2 over position 1 being the most realistic position of the buspirone analogues.

Table 3 also shows that some amino acids are important for ligand binding in only one of the positions. In position 1 (Table 3): Thr81(TMH2) bound to the aromatic moiety of the ligand, Cys119(TMH3) bound to ligand piperazine ring and Ser123(TMH3) bound to ligand aromatic moiety. In postion 2 (Table 3): Phe112 (TMH3) bound to ligand imide moiety, Val117 (TMH3) bound to ligand piperazine ring or aromatic moiety and Phe204(TMH5) bound to ligand piperazine ring. Site directed mutations involving these residues and ligand binding affinity studies of buspirone analogues will clarify the role of these amino acid residues for binding buspirone analogues and further verify the validity of positions 1 and 2.

In the structure of the unbound 5-HT$_{1A}$ receptor, a hydrogen bond between Asp116(TMH3) and Asn386-(TMH7) is present. In position 2, complexes of (1) and (3) had this hydrogen bond broken, but it was present in complexes of (2) and (4). After MD in position 2, the ligands with a quinolinyl moiety ((2) and (4)) were also located closer to the extracellular side than the ligands with a pyrimidinyl moiety (Fig. 5). These positional differences at the ligand binding site, and that the quinolinyl ligands in contrast to the pyrimidinyl ligands were not able to break the hydrogen bond Asp116(TMH3)-Asn386(TMH7), may contribute to the lower affinity of the quinolinyl ligands for the 5-HT$_{1A}$ receptor (Table 1).

A previous molecular modelling study of the 5-HT$_{1A}$ receptor suggested an important role of Ser86(TMH2) for binding a carbonyl group in the imide moiety of buspirone analogues.[37] In the present study, Ser86(TMH2) seemed less important for binding buspirone analogues (Table 3). To verify that Ser86 is not important for ligand binding, contrary to our previous suggestion,[37] we constructed a receptor complex in which a carbonyl group of the imide moiety of (1) was positioned close to Ser86. After energy refinements, the ligand–receptor interaction energy was unfavourable compared with the other complex, indicating that Ser86 is not important for binding of buspirone analgues. Our previous 5-HT$_{1A}$ model was based on the previously suggested general arrangements of TMHs in GPCRs,[38] and TMH3 was less central in the helical bundle compared with the present model. Ser86 was therefore more accessible for ligand interactions in our previous model.

The increase in potential energy of the receptor structure upon ligand binding is higher in position 1 than in position 2, which favours position 2 over position 1 at

the 5-HT$_{1A}$ receptor. After MD in position 2, the rank order of receptor distortion energy upon binding was: (1) < < (3) < (2) < < (4) (Table 6), while the experimental receptor binding affinity decreased in the rank order: (1) < < (3) < (2) ~ (4) (Table 1). Except for compound (4), this indicates that the increase in receptor distortion energy upon binding correlates with a decrease in experimental receptor binding affinities (Table 1), indicating that the high affinity ligands induce a more energetically favourable conformation into the receptor than the low affinity compounds. The structural difference between (1) and (3) is within the imide moiety, indicating that the phthalimide group of compound (3) is the main component for the higher receptor distortion energy of (3) than of (1) upon receptor binding in position 2 (Table 6). In position 2, the imide moiety interacts with several amino acid residues in TMH2, 3 and 7. Table 5 indicates that compounds with a phthalimide group ((3) and (4)) induced larger displacements into TMH2 and 7 than did compounds (1) and (2). The structural difference between (1) and (2) is within the aromatic group, indicating that the quinolinyl moiety of (2) is the main component for the higher receptor distortion energy of (2) than of (1) upon receptor binding (Table 6). The aromatic moiety of the buspirone analogues interacts with several amino acids in TMH3, 5 and 6 (Table 3), with the quinolinyl group of (2) and (4) located closer to the extracellular side than the pyrimidinyl group of (1) and (3) (Fig. 5). Table 5 indicates that compounds with a quinolinyl moiety ((2) and (4)) induced larger displacements into TMH5 and 6 than did (1) and (3). The calculations suggest that the most important determinants for discriminating between the buspirone analogues are repulsive forces between the aromatic ligand moieties and the region around TMH5/TMH6 in the receptor, and between the quinolinyl moiety and the region around TMH2/TMH7 (Fig. 4).

The initial bent conformations of the ligands were changed into an extended conformation during MD in position 1, adopting a conformation close to the crystal structure of 4,4-dimethyl-1-{4-[4-2-quinolinyl)-1-piperazinyl]butyl}-2,6-piperidinedione,[14] while the bent ligand conformations were retained during the simulations with ligands in position 2. Chilmonczyk and co-workers reported that rigid and extended analogues of buspirone exhibit very low affinity towards both 5-HT$_{1A}$ and 5-HT$_{2A}$ serotonin receptors[8] which also suggests that position 2 is more favourable than position 1 at the 5-HT$_{1A}$ receptor.

In aqueous solution, one driving force for binding is the increase in entropy owing to disappearance of ordered water–ligand and water–receptor contacts. This is not taken into account in the present calculations. However, the ligands in the present study are structurally very similar (Table 1) and the entropy contribution to binding is therefore expected to be at a similar level for all the compounds. Moreover, the observed ligand-induced distortion energy and the structural changes of the receptor upon ligand binding favours position 2 over 1 as a more realistic position at the 5-HT$_{1A}$ receptor. Postion 2 is also favoured over 1 based on mutagenesis

data of Asn386(TMH7), and on the ligand conformation in the receptor–ligand complex after MD. However, none of the positions can be categorically excluded as an improper one. The possibilities of more than one binding site for the buspirone analogues, and that the binding site allows some movements of the interacting ligand can not be completely ruled out.

### Buspirone analogues–5-HT$_{2A}$ receptor interactions

During MD with ligands in position 1, the initial bent ligand conformations were changed into more extended structures during MD in position 1 (Fig. 6). However, the ligand conformational changes were not as large as after MD in position 1 at the 5-HT$_{1A}$ receptor. In spite of the receptor-induced changes of ligand conformation in position 1, no significant ligand-induced helical displacements were observed during MD. As seen for the 5-HT$_{1A}$ receptor, the ligand conformations after MD in position 2 were very similar to the initial bent ligand conformation, and none of the ligands adopts such a elongated structure as after MD in positon 1. This may favour position 2 over 1 as the most realistic position at the 5-HT$_{2A}$ receptor, since structure–activity relationship studies have suggested that rigid and extended analogues of buspirone exhibit very low affinity towards both 5-HT$_{1A}$ and 5-HT$_{2A}$ serotonin receptors.[8]

Only minor differences in receptor binding interactions between compound (2) on one side, and the other buspirone analogues on the other side were seen after MD in position 1, while significant differences were seen after MD in position 2. In position 2, compound (2) interacted closer to TMH1 and the N-terminus than did (1), (3) and (4), with the imide moiety interacting strongly with N-terminal amino acids (Val47 and Asp48). Such differences in receptor interactions between (2) on one side, and (1), (3) and (4) at the other side were expected, since the binding affinity of (2) is much lower than of (1) and (4) (Table 1). This may also favour position 2 over position 1 as a more realistic position at the 5-HT$_{2A}$ receptor. The binding affinity of (3) has not been detected (Table 1). However, the receptor interaction mode may suggest that the affinity should be more similar to the value obtained for (1) and (4) than for (2).

### The ligand binding modes at the 5-HT$_{1A}$ and 5-HT$_{2A}$ receptors

The present modelling studies indicate that position 2 was favoured over position 1 as a more realistic position at both the 5-HT$_{1A}$ and the 5-HT$_{2A}$ receptors. In position 2 at both receptor models, the ligand imide moieties interact with amino acids in TMH2 and 7, while the aromatic moieties interact with amino acids in TMH5, 6 and 7, mainly. The protonated amino group in the piperazine ring interacts strongly with the conserved aspartic acid in TMH3 in both receptors. For all ligands at position 2 of the 5-HT$_{1A}$ receptor, the imide group interacts with Leu88(TMH2) and Tyr390(TMH7), while one of the imide carbonyl oxygens forms a hydrogen bond with Ser393(TMH7). The packing of TMH1 and TMH7 relative to each other differs slightly between the

5-HT$_{1A}$ and 5-HT$_{2A}$ receptor models, such that Tyr369(TMH7) is less central in the helical bundle than the corresponding Tyr390(TMH7) in the 5-HT$_{1A}$ receptor, and does not take part in ligand interactions (Table 4). This difference influences the ligand position at the receptor, such that Ser372(TMH7) which corresponds to Ser393(TMH7) of the 5-HT$_{1A}$ receptor, does not form a hydrogen bond with an imide carbonyl group. The differences in the interactions of the imide moieties between the receptors also influence the position of the aromatic moieties relative to the receptor models. In the 5-HT$_{1A}$ receptor, the aromatic ring plane of the buspirone analogues is located perpendicular to the membrane plane, while it is oriented normal to the membrane plane in the 5-HT$_{2A}$ receptor. These differences in ligand binding site architecture between the 5-HT$_{1A}$ and 5-HT$_{2A}$ receptors may contribute to the affinity differences for the buspirone analogues. Ser393/Tyr390 of the 5-HT$_{1A}$ receptor and Ser372/Tyr369 of the 5-HT$_{2A}$ receptor should be experimentally tested for their role in binding to buspirone analogues.

### Conclusion

The present models of the 5-HT$_{1A}$ and 5-HT$_{2A}$ receptors indicated that an asparagine in TMH1 (Asn54 in 5-HT$_{1A}$, Asn92 in 5-HT$_{2A}$), aspartic acid in TMH2 (Asp82 in the 5-HT$_{1A}$ receptor, Asp120 in 5-HT$_{2A}$), a serine in TMH3 (Ser123 in 5-HT$_{1A}$ and Ser162 in 5-HT$_{2A}$), asparagine in TMH7 (Asn396 in 5-HT$_{1A}$, Asn375 in 5-HT$_{2A}$) and proline in TMH7(Pro397 in 5-HT$_{1A}$ and Pro376 in 5-HT$_{2A}$) form interhelical contacts that constrain TMH1, 2, 3 and 7 relative to each others. Simulations of receptor–ligand interactions indicated that the buspirone analogues are not able to cause any significant alteration of the interhelical network upon binding to the 5-HT$_{2A}$ receptor. Upon ligand binding to the 5-HT$_{1A}$ receptor, interhelical hydrogen bonds were broken while others were formed in the region of the highly conserved amino acids in TMH1, 2, 3 and 7. The changes in interhelical hydrogen bonding pattern of the 5-HT$_{1A}$ receptor were followed by rigid body motions of TMH2, 4 and 6 relative to each other and to the other TMHs, and of structural alteration of I2 and I3. These results indicate that conformational changes in the region of highly conserved amino acids in TMH1, 2, 3 and 7 are crucial for ligand-induced receptor activation and proper G-protein interactions. These results are supported by site-directed mutagenesis data.[18–20,25]

The modeling also indicated that ligand imide moieties interact with amino acids in TMH2 and 7, while ligand aromatic moieties interact with amino acids in TMH5, 6 and 7. Further, the main contribution to the affinity differences of the 5-HT$_{1A}$ and 5-HT$_{2A}$ receptors for the buspirone analogues are differences in the packing interactions between TMH1 and 7, which give differences in the receptor geometry in the region of highly conserved serine and tyrosine residues in TMH7. The current models of receptor-ligand interactions might provide a useful approach for further experimental studies of the 5-HT$_{1A}$ and 5-HT$_{2A}$ receptors by protein

engineering experiments. Furthermore, the relatively detailed ligand binding modes emerging from this study may be a useful approach for structure based design of new ligands with an improved receptor selectivity and a possible therapeutical potential.

## Methods

Molecular mechanic energy minimisation (MM) and MD simulations were performed with the AMBER 5.0 all atom force field.[39] Explicit solvent molecules were not included in the calculations, and a distance-dependent dielectric function ($\varepsilon = 4r$, $r$: inter-atomic distance) was used to include the solvent effects. MM energy minimisation of ligand molecules and of averaged receptor–ligand complexes after MD simulations were performed using 0.002 kcal/mol Å for the norm of the energy gradient as convergence criteria. Energy minimisations during the refinement procedure of receptor models were performed by 500 cycles of steepest descents minimisation followed by 2000 cycles of conjugate gradient minimisation. The step-length during MD simulations was 0.001 ps. The cut-off radius for non-bonded interactions during conformational analysis of ligand molecules was 8 Å, while the cut-off radius during energy refinements and MD simulations of receptor models and of receptor–ligand complexes was 12 Å. To preserve the helical conformations of receptor TMHs during MD simulations, constraint forces (corresponding to 5 kcal/mol) were applied between the backbone oxygen atom of residue $n$ and the backbone nitrogen atom of residues $n+4$, excluding prolines, during the MD simulations. Initial simulations indicated that intrahelical constraint forces corresponding to 5 kcal/mol were found to be important for producing rigid helix body motions as observed in experimental studies.[24,25]

### Modeling of ligand molecules

Restrained electric point charges[40] (RESPs) of ligand molecules were calculated quantum mechanically with the Gaussian94 program[41] using an RHF/6-31G* basis set. Molecular-mechanical parameters for all the analogues were initially set equal to standard all-atom AMBER parameters and adjusted to ensure reproduction of the main features of the crystal structure of buspirone (**1**) and 4,4-dimethyl-1-{-4-[4-2-quinolinyl)-1-piperazinyl]butyl}-2,6-piperidinedione.[8]

An initial model of KASPAR (**2**) was constructed from the crystal structure of (**1**). The phthalimide fragment of GL-36 (**3**) and A7 (**4**) was created with the XLeaP program implemented in the AMBER 5.0 software package, while the remaining parts of (**3**) and (**4**) were from the structure of (**1**) and (**2**), respectively. For each compound the nitrogen atom attached to the *n*-butyl moiety was protonated (Table 1). The initial ligand models were energy-minimised and restrained electric point charges[40] (RESPs) were calculated. The generated RESP charges were used for further MM energy minimisations of the ligand molecules. The obtained energy-minimised structures were used to calculate a new set of

RESP charges for each ligand, that was included in a final energy minimisation of the ligands.

Conformational analysis of all the ligands were performed using MD and MM calculations. A set of conformers for each ligand was generated by MD simulation. After an initial equilibrium period started at 0.1 K, MD simulations with velocity scaling were performed at 310 K. The total time of the simulations was 750 ps. The atomic coordinates were saved to disk at 1 ps intervals.

Structural patterns of ligands binding to the 5-HT$_{1A}$ and 5-HT$_{2A}$ receptors were examined and biophore models for ligand binding to the 5-HT$_{1A}$ and 5-HT$_{2A}$ receptors were generated[42] (Fig. 1). The present biophore model of the 5-HT$_{1A}$ receptor is consistent with the pharmacophore model for the 5-HT$_{1A}$ receptor.[14] Conformations obtained during the simulation that fitted the biophore models of the 5-HT$_{1A}$ or 5-HT$_{2A}$ receptors (Fig. 1) were selected and energy minimised. Conformers with a deviation within 1.15 Å in atomic distance between central atoms in the biophore models and corresponding atomic distances in the conformers were energy-minimised.

### Construction of the 5-HT$_{1A}$ receptor model

An initial model of the TMH-bundle was constructed from our previous model of the 5-HT$_{1A}$ receptor.[37] Small changes in the axial rotations and tilting of some of the TMHs were performed to improve the helical packing according to the most recent low resolution structure of frog rhodopsin, and the suggested α-carbon template for the TMHs in the rhodopsin family of GPCRs.[3] This resulted in a TMH-bundle with TMH3 being more central in the helical bundle, and with TMH3 and TMH5 more tilted than in our previous 5-HT$_{1A}$ receptor model.

The N-terminal was copied directly from our previous 5-HT$_{1A}$ receptor model.[37] Initial backbone conformations of the extracellular loops, I1, I2 and the C-terminal were constructed by searching for loop segments in the Protein databank (PDB). The five loop conformations in the database with highest amino acid sequence similarity with each of these receptor segments were inspected visually for the possibility of steric interactions with its local environment in the receptor. The loop conformation with most reasonable interactions and smallest deviation at the terminal ends were selected, and initial structures of the receptor segments were constructed by changing the side chains of the loop conformation into the side chains of the corresponding receptor segment. The PDB identification code for the segments used as initial structures were; I1: 153L, E1: 2EQL, I2: 8CAT, E2: 3CYR, E3: 2REL, and the C-terminal: 2BUS.

The third intracellular loop of the 5-HT$_{1A}$ receptor consists of 113 amino acids. Searching the Protein databank for initial backbone conformations of this loop was not successful, and therefore, this loop needed

special treatment. The Predict-Protein server (www.embl.columbia.edu/pp/submit_adv.html) was used to generate a secondary structure prediction of the loop. α-helical conformation was predicted for residues 4–11 and 93–111, while the segments 37–44 and 61–73 were predicted in β-conformation. Secondary structures of these segments were built according to the prediction. The other segments of I3 were predicted in random conformation, and for this segments the databank was searched for loop structures that was used as initial backbone conformation. A strategy similar to that used for the other intracellular and extracellular loops was used to evaluate possible conformations. The PDB identification code for the chosen segments were; 2BPA, 1BLA and 1NPO. A putative 3-D model of the entire I3 was built from the secondary structure segments and this loop segments. The amphiphilic helices at the N- and C-terminal ends of the loop were densely packed, while the two β conformation regions were packed into a sheet. The side chains of the I3 model were energy refined by 500 cycles of steepest descent minimisation and 2000 cycles of conjugate gradient minimisation while the backbone atoms were kept fixed.

The loops and terminals were connected to the helical bundle and the receptor model was energy refined in several steps: (a) 25 ps of MD simulation at 300 K with the helical bundle at fixed position; (b) 25 ps of MD simulation at 300 K of all side chains in the model; (c) energy minimisation of the entire receptor. A disulfide bridge between Cys109 in TMH3 and Cys187 in E2 was present during all calculations.

### Construction of the 5-HT$_{2A}$ receptor model

The helical bundle of the 5-HT$_{1A}$ receptor model was used as a template to build a model of the helical part of the 5-HT$_{2A}$ receptor by homology. Loops having the same length as corresponding loops in the 5-HT$_{1A}$ receptor (I1, I2, E2 and E3) were also built by homology. Structural templates for the backbone conformations of I3 and E2 and the terminal fragments were taken from the Protein databank. The PDB identification code for the segments used as initial structures were; N-terminal: 1DIL, E1: 1SMD, I3: 1BUR and C-terminus: 2TMD. The loops and terminals were connected to the helical bundle and the 5-HT$_{2A}$ receptor model was refined as described for the 5-HT$_{1A}$ receptor.

### Simulation of receptor–ligand interactions

Results from site directed mutagenesis experiments of the 5-HT$_{1A}$ receptor[29,30,36] were used as a guide to dock the ligands into the 5-HT$_{1A}$ receptor. The selected conformers of (1)–(4) were placed in the central cavity of the receptor model. Several low-energy conformers that fitted the biophore model were considered, and several positions of the ligands relative to the receptor model were considered. In all these positions the protonated amino group of the piperazine ring was close to Asp116 in TMH3. The two positions giving the best structural fit between the receptor and the ligands were considered in detail (positions 1 and 2). In positon 1, the hetero-

aromatic (pyrimidinyl or quinolinyl) moiety was close to Ser123 in TMH3 and Trp358 in TMH6, while in position 2 the heteroaromatic moiety was placed close to Phe204 in TMH5.

The docking of the ligand conformers into the 5-HT$_{2A}$ receptor model was performed as described for the 5-HT$_{1A}$ receptor. Several positions of the ligands relative to the receptor were also considered in the 5-HT$_{2A}$ receptor, but two positions relative to the model seemed most realistic and were considered in detail. In position 1, the heteroaromatic moiety of the ligand was located close to Asp120 (TMH3) and Ser371 (TMH6). In position 2, the heteroaromatic moiety was close to Trp151 (TMH3). The ligand conformers used for MD of receptor–ligand interactions are shown in Figure 3.

All the 16 ligand–receptor complexes were energy-minimised and used as initial structures for 170 ps of MD simulation. The temperature was gradually increased from 0.1 to 300 K during the first 30 ps of the simulations and kept at 300 K between 30 and 170 ps. The 30 coordinate sets saved between 140 and 170 ps were used to calculate average structures of ligand–receptor complexes, which were energy-minimised. The same approach was also used for MD simulations of the free 5-HT$_{1A}$ and 5-HT$_{2A}$ recptor models.

The distortion energy of the 5-HT$_{1A}$ receptor upon ligand binding was calculated for all 5-HT$_{1A}$ receptor-ligand complexes as the difference in potential energy between the receptor structure in the energy-minimised average ligand–receptor complex after MD and the separately energy-minimised receptor structure.

### References

1. Barnes, N. M.; Sharp, T. *Neuropharmacology* **1999**, *38*, 1083.
2. Palczewski, K.; Kumasaka, T.; Hori, T.; Behnke, C. A.; Motoshima, H.; Fox, B. A.; Le Trong, I.; Teller, D. C.; Okada, T.; Stenkamp, R. E.; Yananoto, M.; Miyano, M. *Science* **2000**, *289*, 739.
3. Baldwin, J. M.; Schertler, G. F. X.; Unger, V. M. *J. Mol. Biol.* **1997**, *272*, 144.
4. Traber, J.; Glaser, T. *Trends Pharmacol. Sci.* **1987**, *8*, 432.
5. Goa, K. L.; Ward, A. *Drugs* **1986**, *32*, 114.
6. Bakish, D.; Habin, R.; Hooper, C. L. *CNS Drugs* **1999**, *9*, 271.
7. Peroutka, S. J. *CNS Drugs* **1995**, *4*(Suppl. 1), 18.
8. Chilmonczyk, Z.; Les, A.; Wozniakowska, A.; Cybulski, J.; Koziol, A. E.; Gdaniec, M. *J. Med. Chem.* **1995**, *38*, 1701.
9. Bromidge, S. M.; Dabbs, S.; Davies, D. T.; Duckworth, D. M.; Forbes, I. T.; Ham, P.; Jones, G. E.; King, F. D.; Saunders, D. V.; Starr, S.; Thewlis, K. M.; Wyman, P. A.;

Blaney, F. E.; Naylor, C. B.; Bailey, F.; Blackbourn, T. P.; Holland, V.; Kennett, G. A.; Riley, G. J.; Wood, M. D. *J. Med. Chem.* **1998**, *41*, 1598.

10. Kennett, G. A.; Wood, M. D.; Bright, F.; Cilia, J.; Piper, D. C.; Gager, T.; Thomas, D.; Baxter, G. S.; Forbes, I. T.; Ham, P.; Blackburn, T. P. *Br. J. Pharmacol.* **1996**, *117*, 427.

11. Barret, J. E.; Zhang, L. *Drug Develop. Res.* **1991**, *24*, 179.

12. Hensman, R.; Guimaraes, F. S.; Wang, M.; Deakin, J. F. W. *Psychopharnacology* **1991**, *104*, 220.

13. Kleven, M. S.; Koek, W. *J. Pharmacol. Exp. Ther.* **1996**, *276*, 388.

14. Chilmonczyk, Z.; Szelejewska-Wozniakowska, A.; Cybulski, J.; Cybulski, M.; Koziol, A. E.; Gdaniec, M. *Arch. Pharm. Pharm. Med. Chem.* **1997**, *330*, 146.

15. Henderson, R.; Baldwin, J. M.; Ceska, T. A.; Zemlin, F.; Beckman, E.; Downing, K. H. *J. Mol. Biol.* **1990**, *213*, 899.

16. Pebay-Peyroula, E.; Rummel, G.; Resenbusch, J. P.; Landau, E. M. *Science* **1997**, *277*, 1676.

17. Luecke, H.; Schobert, B.; Richter, H. T.; Cartailler, J. P.; Lanyi, J. K. *J. Mol. Biol.* **1999**, *291*, 899.

18. Zhou, W.; Flanagan, C.; Ballesteros, J. A.; Konvicka, K.; Davidson, J. S.; Weinstein, H.; Millar, R. P.; Sealfon, S. C. *Mol. Pharmacol.* **1994**, *45*, 165.

19. Sealfon, S. C.; Chi, L.; Ebersole, B. J.; Rodie, V.; Zhang, D.; Ballesteros, J. A.; Weinstein, H. *J. Biol. Chem.* **1995**, *270*, 16683.

20. Donnelly, D.; Maudsley, S.; Gent, J. P.; Moser, R. N.; Hurrell, C. R.; Findlay, J. B. *Biochem. J.* **1999**, *339*, 55.

21. Scheer, A.; Fanelli, F.; Costa, T.; De Benedetti, P. G.; Cotecchia, S. *EMBO J.* **1996**, *15*, 3566.

22. Scheer, A.; Fanelli, F.; Costa, T.; De Benedetti, P. G.; Cotecchia, S. *Proc. Natl. Acad. Sci. U.S.A.* **1997**, *94*, 808.

23. Strange, P. G. *T.I.P.S.* **1998**, *19*, 85.

24. Farrens, D. L.; Altenbach, C.; Yang, K.; Hubbel, W. L.; Khorana, H. G. *Science* **1996**, *274*, 768.

25. Liu, J.; Blin, N.; Conklin, B. R.; Wess, J. *J. Biol. Chem.* **1996**, *271*, 6172.

26. Gether, U.; Lin, S.; Ghanouni, P.; Ballesteros, J. A.; Weinstein, H.; Kobilka, B. K. *The EMBO J.* **1997**, *16*, 6737.

27. Schwartz, T. W. *Curr. Opin. Biotech* **1994**, *5*, 434.

28. Hutchins, C. *Endocrine, J.* **1994**, *2*, 7.

29. Chanda, P. K.; Minchin, M. C. W.; Davies, A. R.; Greenberg, L.; Reily, Y.; McGregor, W. H.; Bhat, R.; Lubeck, M. D.; Mitzutani, S.; Huang, P. P. *Mol. Pharmacol.* **1993**, *43*, 516.

30. Ho, B. Y.; Karschin, A.; Branchek, T.; Davidson, N.; Lester, H. A. *FEBS Lett.* **1992**, *312*, 259.

31. Almaula, N.; Ebersole, B. J.; Ballesteros, J. A.; Weinstein, H.; Sealfon, S. C. *Mol. Pharmacol.* **1996**, *50*, 34.

32. Johnson, M. P.; Loncharich, R. J.; Baez, M.; Nelson, D. L. *Mol. Pharmacol.* **1994**, *45*, 277.

33. Johnson, M. P.; Wainscott, D. B.; Lucaites, V. L.; Baez, M.; Nelson, D. L. *Brain Res. Mol. Brain Res.* **1997**, *49*, 1.

34. Roth, B. L.; Shokam, M.; Choudhary, M. S.; Khan, N. *Mol. Pharmacol.* **1997**, *52*, 259.

35. Choudhary, M. S.; Craigo, S.; Roth, B. L. *Mol. Pharmacol.* **1993**, *43*, 755.

36. Guan, X.-M.; Peroutka, S. J.; Kobilka, B. K. *Mol. Pharmacol.* **1992**, *41*, 695.

37. Sylte, I.; Chilmonczyk, Z.; Dahl, S. G.; Cybulski, J.; Edvardsen, Ø. *J. Pharm. Pharmacol.* **1997**, *49*, 698.

38. Baldwin, J. M. *EMBO J.* **1993**, *12*, 1693.

39. Cornell, W. D.; Cieplak, P.; Bayly, C. I.; Gould, I. R.; Merz, K. M., Jr.; Ferguson, D. C.; Spellmeyer, D. C.; Fox, T.; Caldwell, J. W.; Kollmann, P. A. *J. Am. Chem. Soc.* **1995**, *117*, 5179.

40. Cornell, W. D.; Cieplak, P.; Bayly, C. I.; Kollman, P. A. *J. Am. Chem. Soc.* **1993**, *115*, 9620.

41. Frisch, M. J.; Trucks, G. W.; Schlegel, H. B.; Gill, M. P. W.; Johnson, B. G.; Robb, M. A.; Cheeseman, J. R.; Keith, T.; Petersson, G. A.; Montgomery, J. A.; Raghavachari, K.; Al-Laham, M. A.; Zakrzewski, V. G.; Ortiz, J. V.; Foresman, J. B.; Cioslowski, J.; Stefanov, B. B.; Nanayakkara, A.; Challacombe, M.; Peng, C. Y.; Ayala, P. Y.; Chen, W.; Wong, M.W.; Andres, J. L.; Replogle, E.S.; Gomperts, R.; Martin, R.L.; Fox, D. J.; Binkley, J. S.; Defrees, D. J.; Baker, J.; Stewart, W. P.; Head-Gordon, M.; Gonzalez, C.; Pople, J. A. *Gaussian94*, revision D.1; Gaussian, Inc.: Pittsburgh, PA, 1995.

42. Filipek, S. Unpublished results.

43. Titeler, M.; Lyon, R. A.; Davies, K. H.; Glennon, R. A. *Biochem. Pharmacol.* **1987**, *36*, 3265.

44. Hoyer, D.; Schoeffter, P. *J. Recept. Res.* **1991**, *11*, 197.

45. Glennon, R. A.; Naiman, N. A.; Lyon, R. A.; Titeler, M. *J. Med. Chem.* **1988**, *31*, 1968.

46. Szelejewska-Woyniakowsaka, A.; Chilmonczyk, Z.; Cybulski, J.; Cybulski, M. Unpublished results.